

Wiggly Whipped Inflation

Dhiraj Kumar Hazra,^a Arman Shafieloo,^{a,b} George F. Smoot,^{c,d} Alexei A. Starobinsky^{e,f}

^aAsia Pacific Center for Theoretical Physics, Pohang, Gyeongbuk 790-784, Korea

^bDepartment of Physics, POSTECH, Pohang, Gyeongbuk 790-784, Korea

^cParis Centre for Cosmological Physics, APC (CNRS), Université Paris Diderot, Université Sorbonne Paris Cité, 75013 France

^dPhysics Department and Lawrence Berkeley National Laboratory, University of California, Berkeley, CA 94720, USA

^eLandau Institute for Theoretical Physics RAS, Moscow, 119334, Russian Federation

^fKazan Federal University, Kazan 420008, Republic of Tatarstan, Russian Federation

E-mail:

dhiraj@apctp.org, arman@apctp.org, gfsmoot@lbl.gov, alstar@landau.ac.ru

Abstract. Motivated by BICEP2 results on the CMB polarization B-mode which imply primordial gravitational waves are produced when the Universe has the expansion rate of about $H \approx 10^{14}$ GeV, and by deviations from a smooth power-law behavior for multipoles $\ell < 50$ in the CMB temperature anisotropy power spectrum found in the WMAP and Planck experiments, we have expanded our class of large field inflationary models that fit both the BICEP2 and Planck CMB observations consistently. These best-fitted large field models are found to have a transition from a faster roll to the slow roll $V(\phi) = m^2\phi^2/2$ inflation at a field value around $14.6 M_{\text{Pl}}$ and thus a potential energy of $V(\phi) \sim (10^{16} \text{ GeV})^4$. In general this transition with sharp features in the inflaton potential produces not only suppression of scalars relative to tensor modes at small k but also introduces wiggles in the primordial perturbation spectrum. These wiggles are shown to be useful to explain some localized features in the CMB angular power spectrum and can also have other observational consequences. Thus, primordial GW can be used now to make a tomography of inflation determining its fine structure. The resulting Wiggly Whipped Inflation scenario is described in details and the anticipated perturbation power spectra, CMB power spectra, non-Gaussianity and other observational consequences are calculated and compared to existing and forthcoming observations.

Contents

1	Introduction	1
2	CMB Temperature and B-mode Polarization Tension	4
2.1	Necessity to Modify the Power Law Form	4
2.1.1	Running the power law spectral index	4
2.1.2	Broken power law	5
2.1.3	Step in the primordial perturbation spectrum	5
2.1.4	Step in the Inflaton potential	5
2.2	Getting to the Inflation Potential	5
3	Wiggly Whipped Inflationary Scenario	6
3.1	Wiggly Whipped first-Order Transition	6
3.2	Wiggly Whipped second-Order Transition	7
4	Essential numerical details	7
5	Results and discussions	8
5.1	Best fit results	8
5.2	Primordial scalar and tensor perturbation power spectrum	10
5.3	Non-Gaussianity	13
5.4	Matter power spectra	15
5.5	Gravitational Waves	17
6	Conclusions	17

1 Introduction

The recent BICEP2 report [1, 2] of a CMB polarization B-mode signal consistent with the signature of primordial gravitation waves (GW), when combined with previous CMB temperature anisotropy data [3], has two consequences for the inflationary scenario of the early Universe: (1) these GW are produced at the Universe expansion rate $H(t) \equiv \dot{a}(t)/a(t)$ of about 10^{14} GeV in energy units and (2) the inflationary model has to be modified to the extent of adding more parameters beyond the only one required for its simplest realizations. As a result, the concordance model of the contemporary Universe acquires more parameters, too. These are important consequences and their strength depends upon the confirmation and improvement of the BICEP2 results. We proceed under the assumption that the BICEP2 report is essentially correct for the purposes of this paper.

In the context of the inflationary mechanism of primordial gravitational GW production, what ultimately follows from the BICEP2 measurement is the expansion rate $H(t(k))$ for the range of comoving wave vectors k corresponding to the multipoles

$\ell = 30 - 100$ at the time around their first Hubble radius crossing, $k = aH$, during the early quasi-de Sitter (inflationary) stage. Tensor perturbations (to be primordial GW after the second Hubble radius crossing much later, at the radiation or even recent matter dominated stages) arise from quantum vacuum fluctuations of the gravitational field at this stage. Their amplitude is determined by H during inflation, or it can be said, by the de Sitter (Gibbons-Hawking) temperature $T = H/2\pi$, though the energy spectrum of primordial GW after the second Hubble radius crossing is strongly non-thermal that makes possible their detection at cosmological scales very much exceeding the thermal scale of CMB. The power spectrum of primordial metric tensor perturbations generated during the quasi-de Sitter stage, first calculated in [4] where the final answer was presented in the equivalent form of the spectral energy density of GW after the second Hubble radius crossing, is given by

$$P_T(k) \equiv rP_S(k) = \frac{2H(k)^2}{\pi^2 M_{Pl}^2} \quad (1.1)$$

where $H(k)$ is the expansion rate $H(t)$ estimated at the moment when $k = aH$ during inflation and M_{Pl} is the reduced Planck mass, $M_{Pl} = \sqrt{\hbar c/8\pi G} = 2.435 \times 10^{18} \text{ GeV}/c^2$. Using the normalization $P_S = 2.2 \times 10^{-9}$ at the pivot scale $k = 0.05 \text{ Mpc}^{-1}$ (note that GW contribution to CMB anisotropy is negligible for multipoles corresponding to this scale), more precisely we have

$$H(k_*) = 5.0 \times 10^{-5} \left(\frac{r_{0.002}}{0.2} \right)^{1/2} 5^{(0.96-n_S)} M_{Pl} \approx 10^{14} \text{ GeV} \quad (1.2)$$

where $r_{0.002}$ is the tensor-to-scalar ratio at $k_* = 0.002 \text{ Mpc}^{-1}$ and n_S is the scalar perturbation spectral index. $H(k_*)$ determines the characteristic energy scale of inflaton scalar particles and gravitons at the time of their creation. It is much less than the energy density scale $\sim 10^{16} \text{ GeV}$ (the GUT scale) of the inflaton potential that reflects the fact that inflation is “cold”.

Moreover, the inflaton mass during slow-roll inflation should be in turn significantly less than H . In particular, would we restrict ourselves to the $\ell > 50$ CMB anisotropy data from Planck [3] and the CMB polarization B-mode data from BICEP2 [1, 2], then the simplest inflaton model with $V(\phi) = m^2 \phi^2/2$ and the constant inflaton mass $m \approx 2 \times 10^{13} \text{ GeV}$ would produce a very good fit to these data for the standard number of light neutrino species, $N_\nu = 3$ (in this case, $H \approx m\phi/\sqrt{6}M_{Pl}$). So, even in this simplified approach inflation requires inflaton masses much less than the GUT scale.

Now, with the three CMB anisotropy spectra, temperature and E and B-mode polarizations (actually TT, TE, EE, and BB power spectra), we can go much further and determine the inflaton potential $V(\phi)$, its slope and, even more important for particle physicists, the effective inflaton mass, $m_{eff}^2 = V''(\phi)$, irrespective of the knowledge of an underlying microscopic field (string, M-, etc.) theory. In particular, it will be shown in our paper below that taking into account the features in the CMB anisotropy spectrum observed for multipoles $\ell \lesssim 40$ which are of the *same order*, $\sim 10\%$, as the

relative contribution of primordial GW with $r \sim 0.2$ to CMB anisotropy, leads to a whole range of inflaton effective masses from 2×10^{13} GeV to 10^{14} GeV and even more.

The concordance model of cosmology is based on the assumption of the power-law form of the primordial scalar perturbation spectrum and the spatially flat Λ CDM background FLRW model. Though there were hints of deviation from the concordance model since WMAP first year data [5], this model was consistent with the data within uncertainties of observations. With Planck it has been shown that the data indicate significant deviation from the concordance model at small k ($\ell < 50$) [6]. At the same time the data indicate certain localized features in the CMB angular spectrum both for $\ell = 2, 3$ and in the range $20 \lesssim \ell \lesssim 40$. However, the presence of the large scale features could not be confirmed by CMB temperature data alone due to cosmic variance. On the other hand, the BICEP2 data [1, 2], when combined with the Planck temperature data [3], indirectly confirm these large scale features, most importantly a strong suppression in the scalar primordial power spectrum (PPS) in the range $20 \lesssim \ell \lesssim 40$ at more than 3σ [7], since in the presence of primordial GW the required suppression in the scalar spectrum becomes *larger*. This confirmation certainly opens up a possibility to look for particular inflationary models that provides this suppression [7, 8, 11–14]. In [8] we have discussed canonical inflationary models, Whipped Inflation, that can generate the large scale scalar suppression. Afterwards, different inflationary models have been discussed in the context of reconciling Planck and BICEP2 [15–24].

Though there have been efforts to reconcile the observations using an additional neutrino [25] and non-Bunch-Davies vacuum [26] (which effectively changes the low- ℓ power law), we remain firmly convinced that modifying the power law for the low k scalar perturbation spectrum is probably the most likely and reasonable approach which has been discussed in [7, 8].

In this paper, we go a step beyond our work in [8] and naturally extend the scope of the Whipped Inflation potential. Implementing sharp features of the inflaton potential like its (smoothed) step-like behavior or a rapid change of its first derivative into Whipped Inflation, we show that the new models generates oscillations/wiggles along with suppression in the primordial scalar power spectrum at large scales (small k). These oscillations along with the suppression fits the Planck angular power spectrum of temperature anisotropy both at low $\ell < 50$ and high ℓ better than the concordance model of cosmology. The wiggles in the scalar primordial power spectra are imprinted on the matter power spectrum too, which would change the large scale structure observables. From our analysis we identify two models and we estimate the probabilities to detect the features in the scalar primordial power spectrum using large scale structure data from a survey such as Dark Energy Spectroscopic Instrument (DESI) [9, 10] *.

The paper is organized as follows. In Sec. 2 we describe the tension between Planck temperature anisotropy observation and BICEP2 B-mode observation within the context of power law form of the scalar primordial power spectrum and mention the possible ways to reconcile them. In Sec. 3 we provide the Wiggly Whipped Inflation

*DESI is descended from BigBOSS and aimed at obtaining the optical spectra of galaxies and quasars

scenarios, and construct the potential we use in this work. Sec. 4 briefly discusses the essential numerical details used to solve the potential and to compare the scalar and the tensor PPS to the data. Sec. 5 provides the results of our analysis, confronting the proposed theoretical models to the Planck, BICEP2 and other datasets and also discussing the non-Gaussianities generated during inflation. We do also a forecast analysis, deriving the shape of the matter power spectrum for the proposed models comparing them with the expectations of the concordance model and see how well we can distinguish these models from each other using the sensitivity of the future DESI experiment. In Sec. 6 we summarize.

2 CMB Temperature and B-mode Polarization Tension

The Planck observed temperature anisotropy power spectrum is in tension with the BICEP2 B-mode polarization spectrum in the context of the concordance model of Λ CDM with a power-law scalar perturbation spectrum. Planck low- ℓ TT data was previously $\sim 10\%$ lower than the best-fitted model and, if the B-mode polarization is interpreted as tensor modes, then the tensor modes should add low- ℓ temperature anisotropy power. Due to the observed suppressed low- ℓ TT power spectrum, Planck indicates low tensor-to-scalar ratio ($r < 0.11$ at 95% CL) [27], while BICEP2 indicates much higher r (~ 0.2). A reasonable way to address the tension is to bring in features in the scalar primordial power spectrum. This in turn reflects that the single power law form of the primordial spectrum is not supported by the observations. Hence, a modification of the power law scalar PPS becomes necessary.

2.1 Necessity to Modify the Power Law Form

Scalar primordial power spectra can be modified by keeping an eye to the inconsistencies in the datasets that are not addressed by conventional models. Parametrization of the primordial power spectra and model independent reconstruction [28, 29] can reveal the position of the features indicated by the data. We list a few possibilities to address the feature in the scalar PPS from phenomenological and theoretical point of view.

2.1.1 Running the power law spectral index

The power law form of the primordial spectrum, $P_S(k)$, is described by,

$$P_S(k) = A_S(k/k_*)^{n_S-1}, \quad (2.1)$$

where, A_S is the amplitude at the pivot scale k_* and n_S is the tilt of the spectrum. Planck TT data constrains the value $n_S \sim 0.9603 \pm 0.0073$. One can consider allowing the index to vary with k so that $n_S(k) = n_S(k_*) + dn_S(k)/d \ln k$. The running scalar spectral index have been used in order to reconcile the Planck and BICEP2 data [2, 13]. We need sufficiently large running $dn_S/d \ln k \sim -0.02$ in order to match the data which in turn modifies the small scale power as well. To calibrate the small scale power, we then need another degree of freedom (neutrino mass, running of running,

etc.). Running provides an improvement of $-2\Delta \ln \mathcal{L} \sim -6.5$ and indicates that power law scalar PPS is rejected by more than 2σ . However, the data seem just to require a PPS with a suppression in the large scales only, which is achievable by a break in the power law.

2.1.2 Broken power law

Introducing a break in the power spectrum (two different slopes or powers) shows that with one extra parameter the broken the PPS is supported by the data at more than 3σ CL, compared to power law PPS [7]. The broken PPS can provide $-2\Delta \ln \mathcal{L} \sim -12.5$ improvement in fit compared to power law. The extra one degree of freedom makes the PPS substantially more flexible compared to running spectral index without altering small scale power. Theoretically different behavior of scalar field in early and late stages of inflation can describe this phenomenological PPS. With the help of Whipped Inflation we have shown that similar power spectrum is indeed achievable with low level of non-Gaussianities and large tensors [8].

2.1.3 Step in the primordial perturbation spectrum

We [7] and others [11, 12] also showed that a step in the primordial perturbation scalar spectrum would also provide a good fit to the Planck TT power spectrum. We show here a displaced potential at a critical scale can easily produce such a step in the PPS and the results fit the Planck and BICEP2 observations better than a simple fixed power law. If the transition to the displacement is sharp, then there are wiggles introduced to the higher- k modes but these still fit the observations well.

2.1.4 Step in the Inflaton potential

A step in the inflation potential where the power law breaks can generate an intermediate fast-roll phase which can produce localized wiggles in the scalar PPS and the TT angular power spectra [30]. This helps us to fit a few features in the angular power spectra near $\ell = 22$ and 40. In this paper we shall demonstrate that a simple extension of Whipped Inflation can naturally address the large scale suppression that can reconcile Planck and BICEP2 data along with the generation of wiggles in the scalar PPS. The wiggles obtained from the extension can address the localized features in the TT data. This has now become important since from BICEP2, any deviation at large scale power is now more favored than the power law. Moreover, the future polarization data and large scale structure data, with their projected sensitivity, can certainly falsify the existence of these features.

2.2 Getting to the Inflation Potential

Here we outline what we expect from the Inflaton potential in order to satisfy different observables.

1. Suppression of low- ℓ scalars but with large amplitude tensor perturbations.
2. A model that puts a feature on a scale between the horizon to (1/100)'th of the horizon.

3. Resume complete slow roll around $\ell > 100$ and have it persist for an extended ($N > 50$) e-folds.
4. Generate negligible non-Gaussianities [31] or non-Gaussianities that would have been over-looked until now.

To begin with, let us consider the suppression of the low- ℓ scalars but with large tensor perturbations. The scalar power spectrum from Inflation is given by $P_S(k) = A_S k^{n_S-1}$ and the amplitude $P_S(k) \propto V(\phi)^3/V_\phi(\phi)^2$ while for the tensor perturbations $P_T(k) = A_T k^{n_T}$ where the amplitude $P_T \propto H^2 \propto V(\phi)$ where $V(\phi)$ is the inflation potential. To have significant, a la BICEP2, tensors one would need to have a relatively steep potential and thus a large field inflation. However pushing V up would make the scalars go up significantly unless one makes $V_\phi(\phi) \equiv dV/d\phi$ increase by enough more to over compensate and reduce the scalars by the 10 to 15 per cent needed. That takes one from the slow roll regime into the fast roll regime and then one needs to transit to the slow roll regime to get sufficient *e-folds* to generate the full primordial perturbation spectrum and to take care of other issues.

That approach takes care of both points one and two. In order to get to slow roll (point 3) one must then transition to a less steep potential. Hence the need to break the potential from a steep one to a significantly less steep one at a preferred scale to make the transition from the low- $\ell \sim 100$ or low k to the higher ℓ or k portion.

We were concerned that such an abrupt transition would generate significant non-Gaussianity, which is constrained under Planck observations. We were able to make such a model and avoid the significant ringing that generically accompany abrupt features. However, we have since realized that some ringing “wiggles” can actually describe the data more precisely than the more damped versions.

3 Wiggly Whipped Inflationary Scenario

In the paper [8] we had introduced Whipped Inflation potential. In this paper, motivated by possible Whipped Inflation scenarios and keeping an eye to the sharp features in the temperature anisotropy data, we introduce a first order and second order transition in the Whipped inflation potential, which we call Wiggly Whipped Inflaton potential. For similar types of transitions that were discussed in literature, see [32–37].

3.1 Wiggly Whipped first-Order Transition

In this transition we introduce a jump in the potential of the inflaton field *at* the transition (ϕ_0), given by Eq. 3.1.

$$V(\phi) = \gamma\phi^p + \lambda[(\phi - \phi_0)^q + \phi_{01}^q] \Theta(\phi - \phi_0), \quad (3.1)$$

Note that for $\phi_{01} = 0$, the potential simply reduces to the Whipped Inflaton potential that we proposed in the recent paper [8]. Since the field starts rolling from a steeper power law potential and smoothly transits to a flat power law potential, we find a mild

departure from initial slow-roll phase, imprinting a large scale suppression in scalar primordial power spectra. The modified Whipped Inflation potential with a discontinuity ϕ_{01}^q in the potential at ϕ_0 , ensuring a momentary intermediate boost in the kinetic energy of the scalar field during the inflation. The boost imprints wiggles/oscillations in the primordial power spectra. One can certainly expect significantly large non-Gaussianities as well from the model. Since a discontinuity in the potential gives rise to divergent derivative in the potential at the transition, we smooth the discontinuity. We have smoothed the discontinuity using step functions such as $1 + \text{erf}[(\phi - \phi_0)/\Delta]$ and $1 + \tanh[(\phi - \phi_0)/\Delta]$. The features in the primordial scalar power spectrum and the bispectrum depend strongly on the width of the transition Δ . In this paper we have only considered $(p, q) = (2, 3)$ since for Whipped Inflation we obtained best fit in this combination [8].

3.2 Wiggly Whipped second-Order Transition

The second order transition in the inflaton potential originally appeared in [32] for linear potential. Primordial features and non-Gaussianities generated by this inflaton potential have been discussed widely in the literature [38–43]. Since BICEP2 data indicated a large tensor-to-scalar ratio, we revisit similar transition in the context of Whipped Inflation. The potential that we consider in this paper is given by 3.2.

$$V(\phi) = \gamma\phi^p + \lambda\phi^p (\phi - \phi_0) \Theta(\phi - \phi_0), \quad (3.2)$$

Note that, the potential here is continuous at ϕ_0 but not its derivatives. Here also, following the first order transition we smooth the derivative of the potential with a step function of width Δ . Here, we work with $p = 2$, quadratic inflation, we are able to generate appropriate tensor amplitude that is supported by BICEP2 data. The scalar PPS generated in this model comes close to providing a step in the primordial scalar perturbation spectrum.

4 Essential numerical details

Background inflationary equations and the scalar and tensor perturbation equations for the Wiggly Whipped potential are calculated using the publicly available code BI-spectra and Non-Gaussianity Operator, BINGO [41]. Allowing sufficient *e-folds* $\sim 60 - 70$ and by using initial slow roll we fixed the inflaton initial condition. Initial scale factor is estimated assuming that the pivot scale $k_* = 0.05 \text{ Mpc}^{-1}$ leaves the Hubble radius 50 *e-folds* before the end of inflation. We have modified CAMB [44, 45] to work with the BINGO outputs directly. To find the best fit we have Powell’s BOBYQA method of iterative minimization [46] through COSMOMC [47, 48]. The commander and CAMspec likelihood are used to estimate the low- ℓ and high- ℓ likelihood from Planck data [3] respectively. We have used WMAP low- ℓ (2-23) E-mode polarization data [49] (denoted as WP in results section). The complete BICEP2 likelihood is calculated using bandpowers for 9 bins for E and B mode polarization data. We should also mention

here that to make our analysis robust, we have allowed the background cosmological parameters and the 14 Planck foreground nuisance parameters to vary along with the inflationary potential parameters. Note that for Planck, the estimation of the best fit should be done in few steps, since the large number of parameters (inflationary potential parameters + 4 background cosmological parameters + 14 nuisance parameters) often lead the method to a local minima in the parameter space. To get the best fit, we have performed our search by changing the initial starting points in the parameter spaces. In this paper, we shall present two such minima obtained for the first order transition (Eq. 3.1) attempting to fit different features in the angular power spectra. Moreover, it should be noted that since by default `camb` calculates the angular power spectra in few multipoles and interpolate between them, to ensure that the wiggles in the scalar PPS are not missed by the interpolation, we perform our analysis by calculating the angular power spectra in every multipole. The matter power spectra that we present in our analysis for the best fit values of the parameters are also calculated using `camb`. To calculate the non-Gaussianity for this inflationary model, we again use `BINGO` in the equilateral limit. In all our analyses we have assumed spatially flat FLRW Universe. In all our analyses we have assumed spatially flat FLRW Universe. We have defined $M_{\text{Pl}}^2 = 1/(8\pi G)$ and used $\hbar = c = 1$ throughout the paper.

5 Results and discussions

5.1 Best fit results

We start this section by tabulating the best fit results from Wiggly Whipped potential, corresponding to Eq. 3.1 and 3.2 in Table 1. For the first order transition, we provide 2 results corresponding to two minima in the parameter spaces. We note that the width of the step in the first order transition affects the scalar primordial power spectrum severely. Our searches in the parameter space revealed that a relatively smooth step (First order - I) leads to an improvement in the low- ℓ TT angular spectrum from Planck and a sharp transition (First order - II) attempts to fit the high- ℓ glitches in the TT power spectrum, unaddressed by the power law form of scalar PPS. In fact it had been demonstrated in some earlier works [50] that violent oscillations in the scalar primordial power spectrum might help to fit the CMB data better than power law model.

Note that First order - I fits the CMB data from Planck + WP + BICEP2 significantly better ($-2\Delta \ln \mathcal{L} \sim -13.5$) than the power law PPS (for the best fit power law, see [7]). Compared to Whipped Inflation, Wiggly Whipped performs better since the wiggles at the large scale scalar PPS fits the features around $\ell = 22$ and 40. First order - II, on the other hand contains a sharp step in the potential which leads to violent oscillations in the primordial and the angular power spectrum. We find that the minima obtained around the sharp step region does not help to fit the low- ℓ data better and in that sense is not particularly interesting to reduce the tension between Planck and BICEP2. However, compared to power law scalar PPS, this wiggly scalar PPS fits the high- ℓ CAMSpec likelihood better and provides an overall improvement of $-2\Delta \ln \mathcal{L} \sim -8.6$. We should mention that in the first order transition there exist a

Best fit inflation potential (Eqs. 3.1 and 3.2) and cosmological parameters			
	First order - I	First order - II	Second Order
$\Omega_b h^2$	0.022	0.0219	0.0219
$\Omega_{\text{CDM}} h^2$	0.1203	0.1213	0.1205
100θ	1.041	1.04	1.041
τ	0.097	0.085	0.1
γ	2.65×10^{-11}	2.59×10^{-11}	2.68×10^{-11}
λ	2.13×10^{-10}	3.63×10^{-10}	5.2×10^{-13}
ϕ_0 in M_{Pl}	14.66	14.69	14.59
ϕ_{01} in M_{Pl}	0.52	0.18	-
Ω_m	0.32	0.33	0.32
H_0	66.9	66.4	66.8
$-2 \ln \mathcal{L}$ [Best fit]			
commander [-1.13] Planck ($\ell = 2 - 49$)	-13.42	-1.44	-9.67
CAMspec [7797.29] Planck ($\ell = 50 - 2500$)	7795.68	7789.24	7794
WP [2013.38]	2014.34	2013.39	2014.1
BICEP2 [40.04]	39.56	39.8	39.4
Total [9849.58]	9836.16	9841	9837.8
$-2\Delta \ln \mathcal{L}$	-13.42	-8.59	-11.8

Table 1. Best fit parameters for the Wiggly Whipped Inflaton potential Eqs. 3.1 and 3.2. and the best fit cosmological parameters when compared with Planck + WP + BICEP2 data combination. The improvement in fit, $-2\Delta \ln \mathcal{L}$ is obtained upon comparing the χ^2 of the Wiggly Whipped scenario with the power law scalar PPS. The quantities in the square brackets in the likelihood section denotes the best fit likelihood for power law PPS, mentioned in [7].

large degeneracy between the steepness of the potential at the initial stages of inflation (λ) and the extent of the discontinuity in the potential ϕ_{01}^p , which is reflected in the table. However, to explore the complete degeneracy we need to have a full Markov Chain Monte Carlo analysis for the models which is beyond the scope of this paper.

The second order Wiggly Whipped potential provides an overall improvement 12 compared to power law PPS. Interestingly, the improvement comes both from low- ℓ and high- ℓ . Hence, we get improvement both from `commander` and `CAMspec` which is certainly interesting.

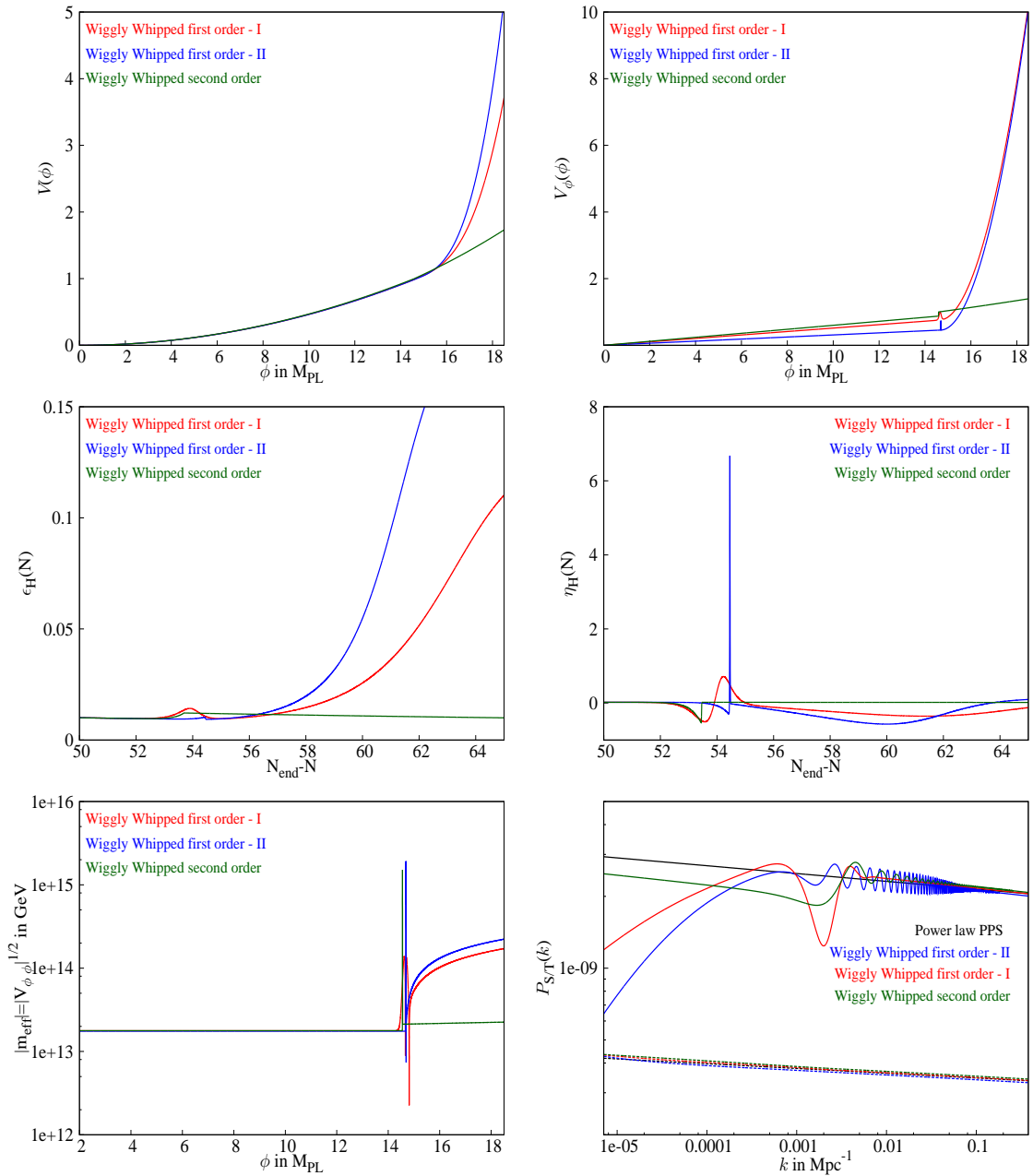


Figure 1. Wiggly Whipped Inflation : [Top]- The best fit potentials (left) and their derivatives (right) corresponding to Eqs. 3.1 and 3.2. [Middle]- The best fit first slow roll parameter (left) and second slow roll parameter (right). [Bottom] The absolute value of effective mass of inflaton (left) and the primordial scalar (solid) and tensors (dashed) power spectra (right).

5.2 Primordial scalar and tensor perturbation power spectrum

In Figure. 1 we plot the relevant quantities for the best fit values denoted in Table 1. At the top left panel we plot the best fit potential for the first and the second order Wiggly Whipped Inflation. Note that for the choice of the power p, q , the first order transition,

at its best fit indicates a steep potential during the early stages of inflation, whereas the second order potential is relatively flat during the complete inflationary phase. The extent of the discontinuity though is not visible in the plot for the potential, it is evident in the slope of the potential plotted to its right. For the First order - I, we find that the derivative of the potential contains kink at the transition with finite width whereas First order - II represents a sharp transition in the slope. The Second order, on the other hand does not reflect a large change in slope but indicates a discontinuity at the transition. The middle left panel contains the first slow roll parameter $\epsilon_H = -\dot{H}/H^2$ for all the three cases for the best fits. Middle right panel contains the second slow roll parameter $\eta_H = d \ln \epsilon_H / dN$. ϵ_H , η_H are plotted as a function of e -folds from the end of inflation N_{end} . We find that First order - I and second order nearly indicates the same time of transition but First order - II chooses an early transition that attempts to fit spurious features in the high- ℓ Planck TT data. The second slow roll parameter clearly distinguishes the different scenarios depending on how the step in the potential and its derivatives are smoothed. The bottom left panel contains the absolute value of effective mass of the inflaton (m_{eff}) as a function of field values. Note that during the slow roll part of the potential all the scenarios suggest the $m_{\text{eff}} \sim 2 \times 10^{13} \text{GeV}$. However during the initial stages of inflation where we break the slow-roll moderately, the inflaton effective mass increase by an order of magnitude (First order case). During the transition, the rapidity of the transition or the sharpness of the step can increase the effective mass to even higher values and it can reach the GUT scale. The primordial scalar and tensor power spectra are plotted in the bottom right panel. First order - I provides a scalar suppression at large scales and at the same time provides a dip around 0.002 Mpc^{-1} and a bump afterwards. However at larger wave-numbers the oscillations soon dies and the scalar PPS converges to a power law form. First order - II, imprints sharp oscillations that continue to the small scales with a decreasing amplitude. Here the dip and the bump in the PPS is not pronounced compared to First order - I around 0.002 Mpc^{-1} . The Second order generates a step in the scalar PPS. The discontinuity in the slope of the potential leads to dip and bump around the same scales as in the case of First order - I and also contains oscillations with decreasing amplitude that continue in small scales like First order - II.

In Figure. 2 we present the angular power spectra ($\mathcal{C}_\ell^{\text{TT}}$) for temperature anisotropy obtained for the three models described above along with the $\mathcal{C}_\ell^{\text{TT}}$ for best fit power law PPS. The Planck data is plotted for the comparison. Note that the Wiggly Whipped Inflation, for all the cases provide suppression in the large scales and at the same time generates wiggles in the angular power spectra which helps to fit the Planck data better than the power law PPS. In the same plot, at the bottom we plot the residual angular power spectra $\Delta \mathcal{C}_\ell^{\text{TT}} = \mathcal{C}_\ell^{\text{TT}}|_{\text{Model/data}} - \mathcal{C}_\ell^{\text{TT}}|_{\text{Power law } \Lambda \text{CDM}}$. In the residual space the features in the data are clearly visible and it is evident that Wiggly Whipped Inflation model for different transitions are sensitive to different features in the data. First order - I provides a scalar suppression at large scales and at the same time fits the drop and excess in power around $\ell \sim 22$ and 40 respectively. First order - II mostly affects the high- ℓ ($\ell \geq 50$) angular power spectrum and it can be seen that violent oscillations around $\ell \sim 200 - 250$, 500 and $750-800$ addresses the features in the data around that

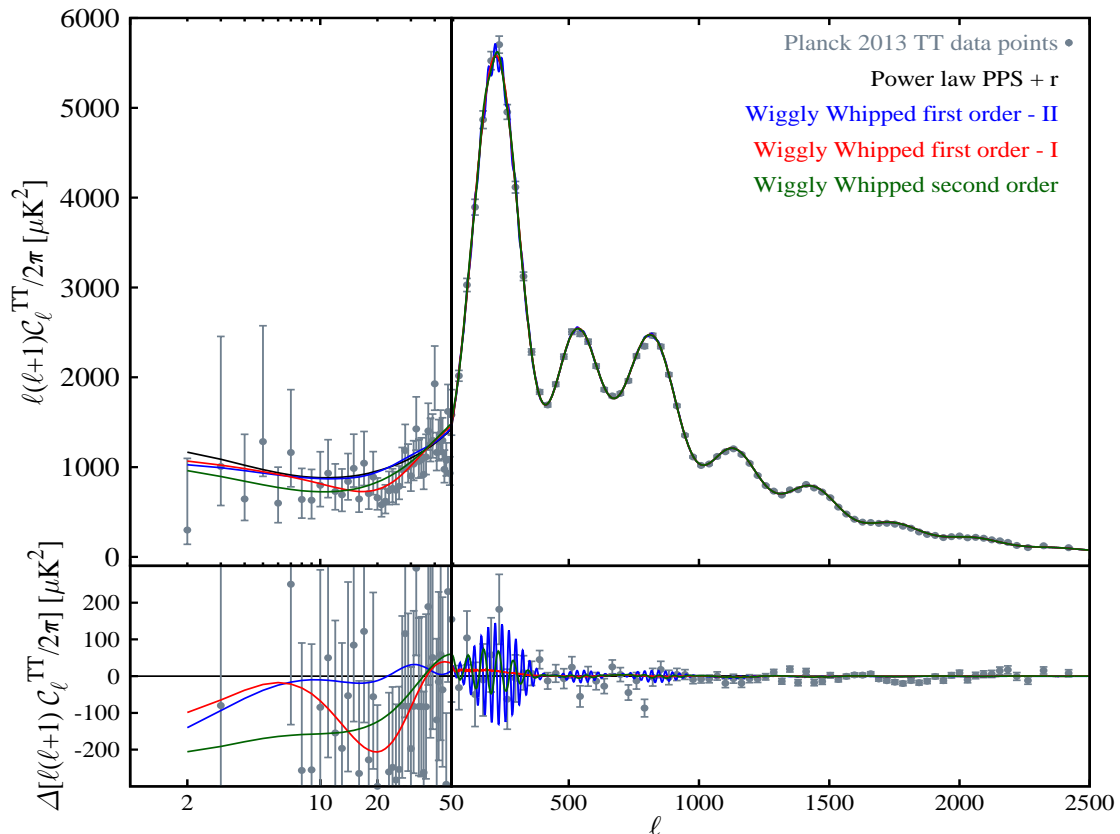


Figure 2. Wiggly Whipped Inflation : Best fit C_ℓ^{TT} plotted for the parameter values quoted in Table 1. At bottom, the $\Delta C_\ell^{\text{TT}}$, residual of the power law ΛCDM best fit model are plotted both for data and the Wiggly Whipped Inflation. Note that in all the cases, Wiggly Whipped Inflation is providing a large scale suppression along with intermediate wiggles in the angular power spectra.

region, which is unaddressed by the power law ΛCDM model. Second order Wiggly Whipped potential provides the strongest suppression in the C_ℓ^{TT} at large scales and attempts to fit $\ell \sim 22$ and 40 features. Around the first CMB peak, the second order also introduces oscillations which again helps to fit the data better. However, afterwards the amplitude of the oscillations decreases which makes the smaller scale C_ℓ^{TT} very similar to the one obtained from power law PPS.

In Figure 3, for the same models we plot the polarization power spectra, *i.e.*, $C_\ell^{\text{TE/EE/BB}}$. The data points from WMAP 9 year observations and BICEP2 observations are also plotted. Note that large scale suppression in scalar PPS are also reflected in TE/EE polarization data. Compared to WMAP-9 it is clear that BICEP2 data points are much closer to the model predictions in all the cases. From the plot of C_ℓ^{BB} , it is clear that all these models are able to fit the B-mode data to similar extent. We must mention here that though the wiggles in the First order - II address the TT data better than power law, there is a possibility that these oscillations fit noise in the angular power spectrum. However, similar features in the polarization spectrum

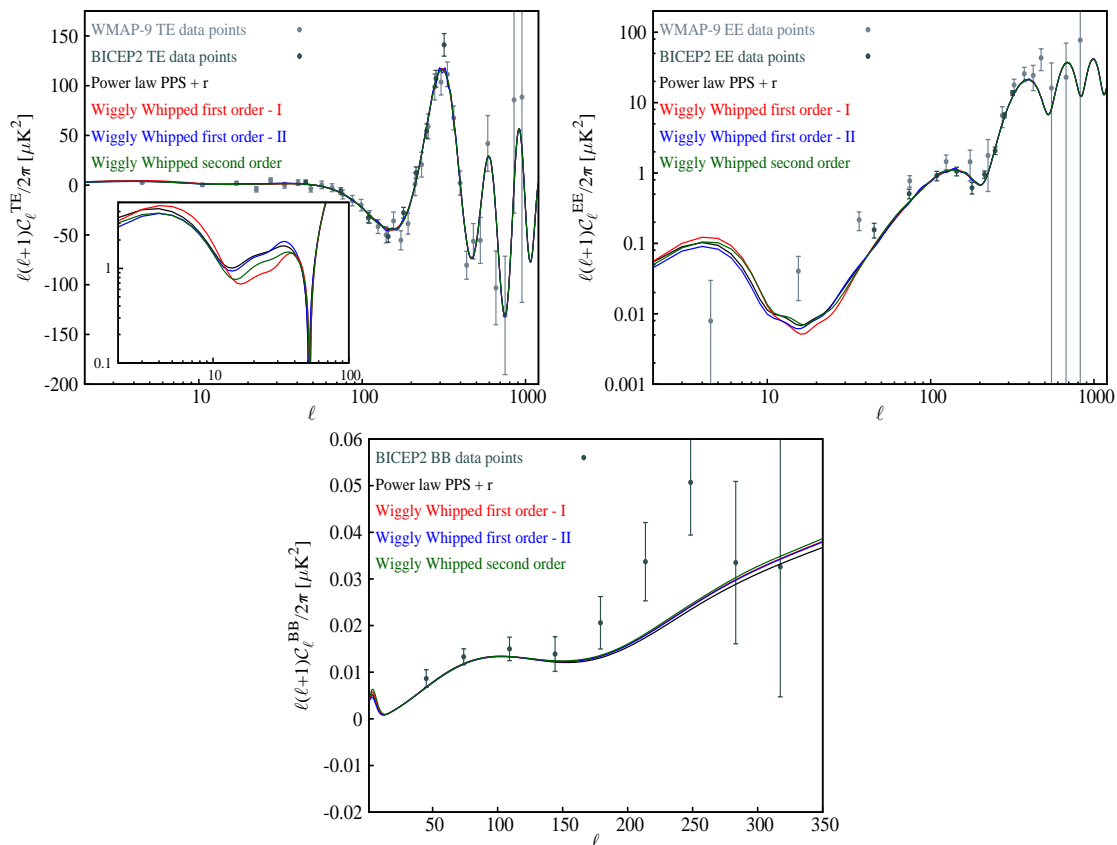


Figure 3. Wiggly Whipped Inflation : TE (top left), EE (top right) and BB (bottom) polarization angular power spectra for different models and the data from WMAP-9 and BICEP2 are plotted. In the top left panel, the inset contains the absolute values of TE angular power spectra.

will help us to distinguish real features from the random fluctuations. We expect with Planck polarization data, we shall be able hunt down the features in the data with much higher confidence.

5.3 Non-Gaussianity

Along with the power spectra which represents the two point correlations of perturbations, we have constraints on the bispectrum from the Planck bispectrum measurements. Based on Maldacena formalism [51] and following the methods described in [29, 39, 41, 52] we use the publicly available code BINGO to calculate the bispectrum, specifically the local f_{NL} in equilateral triangular configuration [†] for the Wiggly Whipped Inflation. The constraints on primordial non-Gaussianity has been found to

[†]Local f_{NL} can be derived from bispectrum $\mathcal{B}_s(\mathbf{k}_1, \mathbf{k}_2, \mathbf{k}_3)$ as

$$f_{\text{NL}}(\mathbf{k}_1, \mathbf{k}_2, \mathbf{k}_3) = -\frac{10}{3} (2\pi)^{-4} (2\pi)^{9/2} k_1^3 k_2^3 k_3^3 \mathcal{B}_s(\mathbf{k}_1, \mathbf{k}_2, \mathbf{k}_3) \times [k_1^3 P_s(k_2) P_s(k_3) + \text{two permutations}]^{-1}$$

and we use $k_1 = k_2 = k_3 = k$ for equilateral triangular case.

be $f_{\text{NL}} = 2.7 \pm 5.8$. For Whipped Inflation we have demonstrated that f_{NL} is $\mathcal{O}(0.1-0.2)$ which is certainly favored by Planck data.

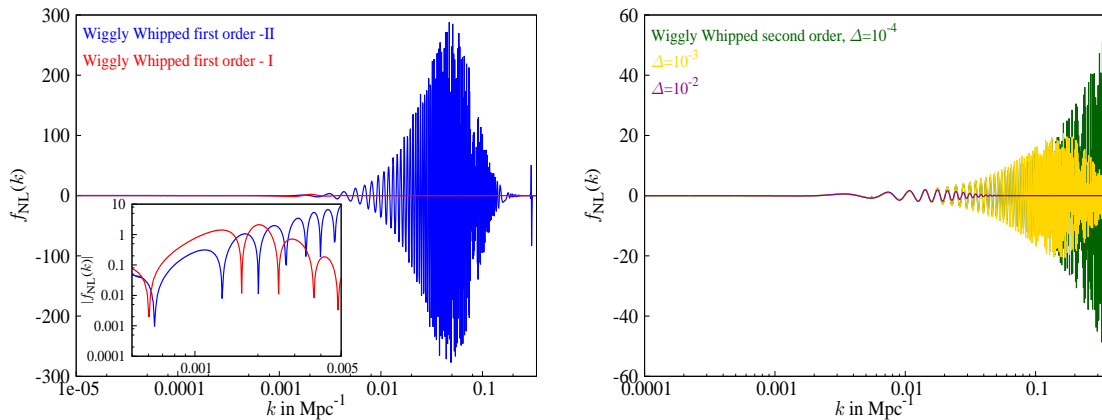


Figure 4. Wiggly Whipped Inflation : Bi-spectrum, specifically the f_{NL} plotted in equilateral triangular configuration. [Left] The f_{NL} plotted for two first order transitions. [Right] The f_{NL} plotted for the second order transition. For the second order transition, we plot the f_{NL} for different smoothing width of the transition or equivalently for different time taken by the scalar field during the transition.

However, for Wiggly Whipped Inflation one can expect higher non-Gaussianity due to sharp departures from slow roll. We present the f_{NL} for the first order and second order Wiggly Whipped potentials in Figure 4. In left panel we plot the f_{NL} for First order - I and II cases. In the right panel we plot the Second order case with different widths of smoothing. For the First order - I case, we find that the f_{NL} is $\mathcal{O}(2-3)$ and for First order - II case, due to violent oscillations the f_{NL} is boosted up to $\mathcal{O}(300)$. The inset of the left plot contains the absolute value of f_{NL} to demonstrate the order of magnitude difference in these two first order transitions.

For the Second order Wiggly Whipped potential, we know that the discontinuity in the slope of the potential does not affect the primordial spectrum significantly but since f_{NL} contains second derivative of the potential, which contains a Dirac Delta function, for an instantaneous transition this model generates a linearly divergent bispectrum for this model as has been shown before [41–43]. However, as have been argued in [42, 43], for any physically plausible transition, which occurs in a finite time, the bispectrum ceases to be divergent. This statement also holds true for the First Order -I and II, however, since the power spectrum in the first order transition is directly related to the smoothness of the step, we plot the bispectrum for the best fit smoothing width. In the Second order case we plot the f_{NL} for three different smoothing width Δ (here Δ denotes the width in field space in M_{Pl}). We note that for a very sharp transition, $\Delta = 10^{-4}$ the f_{NL} becomes linearly divergent, while for $\Delta = 10^{-3}$ we find f_{NL} reaches a maximum value of 20 and then decreases, as has also been shown in [43]. For even smoother transition ($\Delta = 10^{-2}$), we find f_{NL} becomes $\mathcal{O}(2)$ at its peak [‡]. We should

[‡]For a recent discussion on bispectra generated in the models with discontinuity in the derivatives

mention that for these values of Δ , the primordial power spectra and hence the angular power spectra remains unaffected.

Now, the question is whether the large values of the primordial bispectra are supported by the Planck data. To answer this we need to compare the angular bispectra obtained from these models with the Planck bispectrum data. From a first look, it may be argued that since the violent oscillations in the primordial power spectrum leads to a large and oscillating f_{NL} , in a finite bin width of Planck resolution the f_{NL} will be averaged out. However, to have a full understanding of the issue, we need to wait for Planck polarization data to confirm the oscillations in Wiggly Whipped First order - II case and then compare the bispectrum directly. Till then we can at least say that Wiggly Whipped First order - I and Second order (for a smooth transition) are completely consistent with Planck bounds.

5.4 Matter power spectra

Features in the primordial power spectra that are not located only in the large scales can alter the matter power spectrum in the observable range of recent and future large scale structure data. Wiggly Whipped Inflation introduces wiggles in the primordial power spectra that are not just located in the largest scales. Due to the non-local nature of the wiggles, in future it might be possible to identify and constrain them from matter power spectra data from DESI with high confidence. In Fig. 5, we provide the matter power spectra for the Wiggly Whipped potentials (Eqs. 3.1 and 3.2) for the best fit values of the potentials and the corresponding cosmological parameters provided in Table 1. The left panel of the Fig. 5 contains the matter power spectra for different models and right panel contains the ratio of matter power spectra for different Wiggly Whipped models with respect to the matter power spectrum obtained from power law scalar PPS. Note that the First Order-I and the Second Order case imprints oscillations affecting a broad range from the very large scales till the baryon acoustic oscillations scales. This long range deviation from the expectations of the power-law PPS might be detectable by the future large scale structure surveys such as DESI [10].

The fractional error estimates from for DESI [§] are provided in the right panel. Note that we have overlaid the errors on the Second Order transition, since this model provides a long range oscillations with sufficiently large width for detection. For the First Order - I, the large scale dip might be also well constrained with DESI. Independent detection of such large scale features with DESI would significantly increase confidence in the Wiggly Whipped scenarios as a robust model of inflation especially if CMB data continues to fit these models well. Second Order model contains both the large scale dip and oscillations extending till BAO scale and it will probably be more tightly constrained since around BAO scales we shall have more control on the data due to low cosmic variance and large amount of cleaner data. Note that both First Order -I and the Second Order Wiggly Whipped is showing an excess in power at small scales compared to power law PPS. This is happening due to the fact that

of the potential, see [43, 53]

[§]Private communication with Pat Mc Donald.

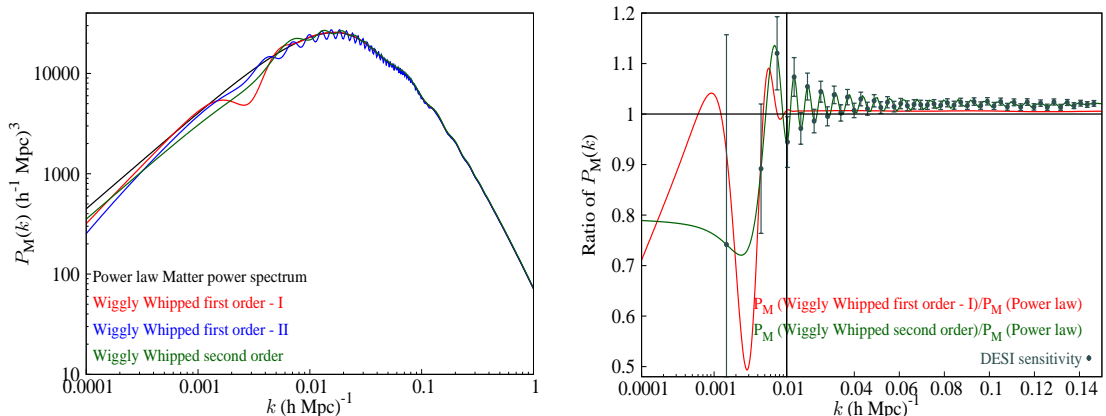


Figure 5. Wiggly Whipped Inflation : Matter power spectra (left) obtained from the best fit potential and background parameters (in Table 1) and the ratio (right) *w.r.t.* the matter power spectra obtained from power law best fit model. The DESI forecasted fractional errors are overlayed in the right panel as well. Note that from the future matter power spectrum data we shall be able to identify specific features in the primordial power spectrum.

the best fit parameters are obtained only from CMB data, where no large scale matter power spectra data has been used.

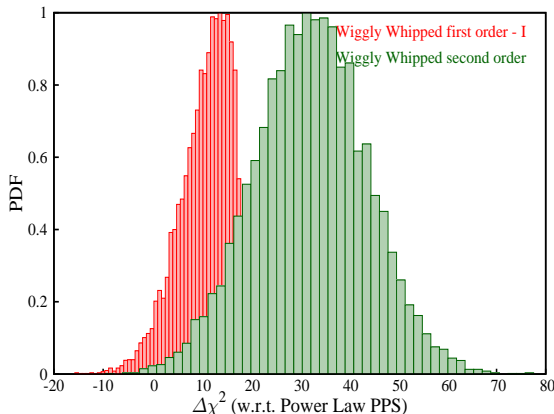


Figure 6. Probability distribution function of $\Delta\chi^2 = -2 [\ln[\mathcal{L}_{\text{Power law}}] - \ln[\mathcal{L}_{\text{Wiggly Whipped fiducial}}]]$ for the two cases of Wiggly Whipped first order - I and Wiggly Whipped second order are plotted. 10000 realizations of the future DESI binned matter power spectrum data have been used in these simulations. One can clearly see that the future matter power spectrum data will be sensitive to the features of the primordial spectrum providing us additional hints towards deviations from the standard power-law form of the PPS.

In order to have a quantitative estimate of the expected sensitivity of DESI towards determining the features in the scalar PPS, we generate 10000 mock data using the projected errors in different scales based on two fiducial models. We have used Wiggly Whipped first order - I and second order as fiducial models since these two models have features which will not be averaged out in a detectable bin width.

For the 10000 data realizations we obtain the likelihood from the corresponding fiducial model ($\ln[\mathcal{L}_{\text{Wiggly Whipped fiducial}}]$) and the power law ($\ln[\mathcal{L}_{\text{Power law}}]$) allowing an overall amplitude shift. The probability distribution function (PDF) of the likelihood difference $\Delta\chi^2 \equiv -2\Delta\ln[\mathcal{L}] = -2[\ln[\mathcal{L}_{\text{Power law}}] - \ln[\mathcal{L}_{\text{Wiggly Whipped fiducial}}]]$ is plotted in Fig 6. One can see that the future matter power spectrum large scale structure data can indeed distinguish the Wiggly Whipped second order model and power-law with a very high confidence. It is also evident that the future matter power spectrum data can give us clear hints for the case of Wiggly Whipped first order - I or any similar case deviating from the expectations of the power-law form of the PPS.

5.5 Gravitational Waves

We have calculated the inflationary gravitational wave spectrum for our models and shown them in the bottom right panel of Figure 1. As can be seen they are tilted red relative to scale invariant spectrum, which implies that they would be detectable by BBO (Big Bang Observer) but not by eLISA [54] or LIGO [55] II or III. Thus, if these models continue to fit new observations, the interest in BBO gravitational wave detector becomes more strongly motivated.

6 Conclusions

In this paper we explored a range of variations for the Whipped inflation scenario that we had discussed in a recent paper [8] in the light of Planck and BICEP2. Introducing a discontinuity in the potential and/or its first derivative at the transition point of the Whipped Inflation potentials, we have shown that in general sharp time or field value structures in the inflaton potential introduce Wiggles in the primordial power spectrum as one would expect. These wiggles can be supported by the CMB TT angular power spectrum data from Planck. Apart from reconciling the Planck and BICEP2 data with a large scale scalar suppression, Wiggly Whipped Inflation models go one step further and addresses features in the TT data from Planck. A discontinuous step introduces an instantaneous transition in the field value or potential, which might result in divergent two point and three point correlation function of curvature perturbations. For a realistic transition we model the discontinuity with a smoothed step in the inflaton potential (WWI type I, or first order) or by a rapid change of its first derivative (WWI type II, or second order). By comparing with Planck and BICEP2 data we show that in both the cases we get significant improvement in likelihood compared to power law scenario. For two different smoothing widths we obtain two different kinds of scalar PPS ; one of which fits the low- ℓ broad features and the other attempts to fit features in the high- ℓ Planck TT data.

These best-fitted large field models are found to have a transition from a faster roll to the slow roll $V(\phi) = (1/2)m^2\phi^2$ inflation at a field value around $14.6M_{\text{Pl}}$ and thus a potential energy of $V(\phi) \sim (10^{16} \text{ GeV})^4$. In general this transition and any features in the large field potential produces not only suppression of scalars relative to tensor modes at small k but also introduces wiggles in the primordial perturbation

spectrum. These wiggles can help fitting localized features in the CMB angular power spectrum and can affect other cosmological observables too.

On the other hand, the WWI type II introduces large-scale scalar suppression by generating a step in the large scale TT spectrum. Along with the step this model also introduces oscillations in the intermediate scales. This step and the oscillations helps to fit both the large and intermediate scale temperature data from Planck significantly better than the power law scalar PPS. The presence and importance of such wiggles/oscillations can be tested by the future polarization data as well. In this regard Planck polarization data can be very insightful. We should note that for the purpose of cosmological parameter estimation using other CMB observations such as B-mode polarization data from POLARBEAR [56] and SPT [57] can be also very useful. We also calculated the extent of non-Gaussianities, especially the bispectra in these models and we found that for the models we considered, for a finite-time transition, the f_{NL} is consistent with Planck bounds. For a very sharp transition, where the f_{NL} is large but oscillating rapidly around zero, the agreement with the data needs to be checked with more carefully binned Planck bispectrum data.

Moreover, we also present the matter power spectrum in these models at their best fit values. Using the forecasted errors from DESI, we argue that the matter power spectrum constraints will certainly be able to confirm the existence of the wiggly features in the primordial power spectrum if they are really present. If such models become highly favored by the data then one can think of next generation of large scale structure surveys to provide improved sensitivity to the low- k region.

Here we can summarize that with the full set of CMB temperature and E and B-mode polarization anisotropy spectra, we can determine the inflaton potential, its slope and, most importantly for particle physicists, the effective inflaton mass without needing to know the underlying microscopic field (string, M-, etc.) theory. In particular, in WWI this mass, while being almost constant and $\sim 2 \times 10^{13}$ during the last 50 e -folds of inflation, grows and becomes of the order of 10^{14} GeV and higher when the inflaton field reaches the value $\phi = \phi_0$ where its potential has a sharp feature. We have shown that around the sharp feature the effective mass of inflation can reach the GUT scale depending on the rapidity of the transition. All this follows from cosmological observational data, leaving to theoreticians to extract this complicated and fine mass spectrum from particle physics at such high energies.

Acknowledgments

D.K.H. and A.S. wish to acknowledge support from the Korea Ministry of Education, Science and Technology, Gyeongsangbuk-Do and Pohang City for Independent Junior Research Groups at the Asia Pacific Center for Theoretical Physics. G.F.S. acknowledges the financial support of the UnivEarthS Labex program at Université Sorbonne Paris Cité (ANR-10-LABX-0023 and ANR-11-IDEX-0005-02). We thank Pat McDonald for providing the DESI matter power spectrum error estimates. We also acknowledge the use of publicly available CAMB and COSMOMC in our analysis. The authors would like to thank Antony Lewis for providing us the new COSMOMC pack-

age that takes into account the recent BICEP2 data. We acknowledge the use of WMAP-9 data and from Legacy Archive for Microwave Background Data Analysis (LAMBDA) [58], Planck data and likelihood from Planck Legacy Archive (PLA) [59] and BICEP2 data from [60]. A.S. would like to acknowledge the support of the National Research Foundation of Korea (NRF-2013R1A1A2013795). A.A.S. was partially supported by the grant RFBR 14-02-00894.

References

- [1] P. A. R. Ade *et al.* [BICEP2 Collaboration], arXiv:1403.4302 [astro-ph.CO].
- [2] P. A. R. Ade *et al.* [BICEP2 Collaboration], arXiv:1403.3985 [astro-ph.CO].
- [3] P. A. R. Ade *et al.* [Planck Collaboration], arXiv:1303.5075 [astro-ph.CO].
- [4] A. Starobinsky, JETP Lett. **30**, 682 (1979).
- [5] H. V. Peiris *et al.* [WMAP Collaboration], *Astrophys. J. Suppl.* **148**, 213 (2003) [astro-ph/0302225].
- [6] D. K. Hazra and A. Shafieloo, *JCAP* **01**, 043 (2014) [arXiv:1401.0595 [astro-ph.CO]].
- [7] D. K. Hazra, A. Shafieloo, G. F. Smoot and A. A. Starobinsky, arXiv:1403.7786 [astro-ph.CO].
- [8] D. K. Hazra, A. Shafieloo, G. F. Smoot and A. A. Starobinsky, arXiv:1404.0360 [astro-ph.CO].
- [9] M. Levi *et al.* [DESI Collaboration], arXiv:1308.0847 [astro-ph.CO].
- [10] See <http://desi.lbl.gov>.
- [11] C. R. Contaldi, M. Peloso and L. Sorbo, arXiv:1403.4596 [astro-ph.CO].
- [12] V. c. Miranda, W. Hu and P. Adshead, arXiv:1403.5231 [astro-ph.CO].
- [13] K. N. Abazajian, G. Aslanyan, R. Easther and L. C. Price, arXiv:1403.5922 [astro-ph.CO].
- [14] B. Hu, J. -W. Hu, Z. -K. Guo and R. -G. Cai, arXiv:1404.3690 [astro-ph.CO].
- [15] M. Kawasaki, T. Sekiguchi, T. Takahashi and S. Yokoyama, arXiv:1404.2175 [astro-ph.CO].
- [16] B. Freivogel, M. Kleban, M. R. Martinez and L. Susskind, arXiv:1404.2274 [astro-ph.CO].
- [17] R. Bousso, D. Harlow and L. Senatore, arXiv:1404.2278 [astro-ph.CO].
- [18] H. Firouzjahi and M. H. Namjoo, arXiv:1404.2589 [astro-ph.CO].
- [19] W. H. Kinney and K. Freese, arXiv:1404.4614 [astro-ph.CO].
- [20] J. P. Zibin, arXiv:1404.4866 [astro-ph.CO].
- [21] A. Achucarro, V. Atal, B. Hu, P. Ortiz and J. Torrado, arXiv:1404.7522 [astro-ph.CO].
- [22] J. E. Kim, arXiv:1405.0221 [hep-th].
- [23] R. Kallosh, A. Linde and A. Westphal, arXiv:1405.0270 [hep-th].

- [24] S. Mukohyama, R. Namba, M. Peloso and G. Shiu, arXiv:1405.0346 [astro-ph.CO].
- [25] J. -F. Zhang, Y. -H. Li and X. Zhang, arXiv:1403.7028 [astro-ph.CO]; C. Dvorkin, M. Wyman, D. H. Rudd and W. Hu, arXiv:1403.8049 [astro-ph.CO].
- [26] A. Ashoorioon, K. Dimopoulos, M. M. Sheikh-Jabbari and G. Shiu, arXiv:1403.6099 [hep-th].
- [27] P. A. R. Ade *et al.* [Planck Collaboration], arXiv:1303.5082 [astro-ph.CO].
- [28] S. Hannestad, Phys. Rev. D **63** (2001) 043009 [astro-ph/0009296]; M. Tegmark and M. Zaldarriaga, Phys. Rev. D **66** (2002) 103508 [astro-ph/0207047]; S. L. Bridle, A. M. Lewis, J. Weller and G. Efstathiou, Mon. Not. Roy. Astron. Soc. **342** (2003) L72 [astro-ph/0302306]; A. Shafieloo and T. Souradeep, Phys. Rev. D **70** (2004) 043523 [astro-ph/0312174]; P. Mukherjee and Y. Wang, Astrophys. J. **599** (2003) 1 [astro-ph/0303211]; D. Tocchini-Valentini, Y. Hoffman and J. Silk, Mon. Not. Roy. Astron. Soc. **367** (2006) 1095 [astro-ph/0509478]; N. Kogo, M. Sasaki and J. 'i. Yokoyama, Prog. Theor. Phys. **114** (2005) 555 [astro-ph/0504471]; S. M. Leach, Mon. Not. Roy. Astron. Soc. **372** (2006) 646 [astro-ph/0506390]; A. Shafieloo and T. Souradeep, Phys. Rev. D **78** (2008) 023511 [arXiv:0709.1944 [astro-ph]]; P. Paykari and A. H. Jaffe, Astrophys. J. **711** (2010) 1 [arXiv:0902.4399 [astro-ph.CO]]; G. Nicholson and C. R. Contaldi, JCAP **0907**, 011 (2009) [arXiv:0903.1106 [astro-ph.CO]]; C. Gauthier and M. Bucher, JCAP **1210**, 050 (2012) [arXiv:1209.2147 [astro-ph.CO]]; R. Hlozek, J. Dunkley, G. Addison, J. W. Appel, J. R. Bond, C. S. Carvalho, S. Das and M. Devlin *et al.*, Astrophys. J. **749** (2012) 90 [arXiv:1105.4887 [astro-ph.CO]]; J. A. Vazquez, M. Bridges, M. P. Hobson and A. N. Lasenby, JCAP **1206**, 006 (2012) [arXiv:1203.1252 [astro-ph.CO]]; D. K. Hazra, A. Shafieloo and T. Souradeep, JCAP **1307**, 031 (2013) [arXiv:1303.4143 [astro-ph.CO]]; D. K. Hazra, A. Shafieloo and T. Souradeep, Phys. Rev. D **87**, 123528 (2013) [arXiv:1303.5336 [astro-ph.CO]]; P. Hunt and S. Sarkar, arXiv:1308.2317 [astro-ph.CO]; S. Dorn, E. Ramirez, K. E. Kunze, S. Hofmann and T. A. Ensslin, JCAP **1406**, 048 (2014) [arXiv:1403.5067 [astro-ph.CO]].
- [29] D. K. Hazra, A. Shafieloo and G. F. Smoot, JCAP **1312**, 035 (2013) arXiv:1310.3038 [astro-ph.CO].
- [30] J. A. Adams, B. Cresswell and R. Easther, Phys. Rev. D **64** (2001) 123514 [astro-ph/0102236]; R. Allahverdi, K. Enqvist, J. Garcia-Bellido and A. Mazumdar, Phys. Rev. Lett. **97** (2006) 191304 [hep-ph/0605035]; L. Covi, J. Hamann, A. Melchiorri, A. Slosar and I. Sorbera, Phys. Rev. D **74** (2006) 083509 [astro-ph/0606452]; R. K. Jain, P. Chingangbam, J. -O. Gong, L. Sriramkumar and T. Souradeep, JCAP **0901** (2009) 009 [arXiv:0809.3915 [astro-ph]]; M. J. Mortonson, C. Dvorkin, H. V. Peiris and W. Hu, Phys. Rev. D **79** (2009) 103519 [arXiv:0903.4920 [astro-ph.CO]]; D. K. Hazra, M. Aich, R. K. Jain, L. Sriramkumar and T. Souradeep, JCAP **1010**, 008 (2010) [arXiv:1005.2175 [astro-ph.CO]]; V. Miranda, W. Hu and P. Adshead, Phys. Rev. D **86**, 063529 (2012) [arXiv:1207.2186 [astro-ph.CO]]; M. Benetti, arXiv:1308.6406 [astro-ph.CO].
- [31] P. A. R. Ade *et al.* [Planck Collaboration], arXiv:1303.5084 [astro-ph.CO].
- [32] A. A. Starobinsky, JETP Lett. **55**, 489 (1992).
- [33] A. D. Linde, Phys. Rev. D **59**, 023503 (1999) [hep-ph/9807493].

- [34] A. D. Linde, M. Sasaki and T. Tanaka, Phys. Rev. D **59**, 123522 (1999) [astro-ph/9901135].
- [35] M. Joy, V. Sahni, A. A. Starobinsky, Phys. Rev. D **77**, 023514 (2008) [arXiv:0711.1585].
- [36] M. Joy, A. Shafieloo, V. Sahni, A. A. Starobinsky. JCAP **0906**, 028 (2009) [arXiv:0807.3334].
- [37] R. Bousso, D. Harlow and L. Senatore, arXiv:1309.4060 [hep-th].
- [38] Y. -i. Takamizu, S. Mukohyama, M. Sasaki and Y. Tanaka, JCAP **1006**, 019 (2010) [arXiv:1004.1870 [astro-ph.CO]].
- [39] J. Martin and L. Sriramkumar, JCAP **1201**, 008 (2012) [arXiv:1109.5838 [astro-ph.CO]].
- [40] F. Arroja, A. E. Romano and M. Sasaki, Phys. Rev. D **84**, 123503 (2011) [arXiv:1106.5384 [astro-ph.CO]].
- [41] D. K. Hazra, L. Sriramkumar and J. Martin, JCAP **1305**, 026 (2013) [arXiv:1201.0926 [astro-ph.CO]].
- [42] F. Arroja and M. Sasaki, JCAP **1208**, 012 (2012) [arXiv:1204.6489 [astro-ph.CO]].
- [43] J. Martin, L. Sriramkumar and D. K. Hazra, arXiv:1404.6093 [astro-ph.CO].
- [44] See, <http://camb.info/>.
- [45] A. Lewis, A. Challinor and A. Lasenby, Astrophys. J. **538** (2000) 473 [astro-ph/9911177].
- [46] M. J. D. Powell, Cambridge NA Report NA2009/06, University of Cambridge, Cambridge (2009).
- [47] See, <http://cosmologist.info/cosmomc/>.
- [48] A. Lewis and S. Bridle, Phys. Rev. D **66** (2002) 103511 [astro-ph/0205436].
- [49] G. Hinshaw, D. Larson, E. Komatsu, D. N. Spergel, C. L. Bennett, J. Dunkley, M. R.olta and M. Halpern *et al.*, arXiv:1212.5226 [astro-ph.CO].
- [50] T. Biswas, A. Mazumdar and A. Shafieloo, Phys. Rev. D **82**, 123517 (2010) [arXiv:1003.3206 [hep-th]]; R. Flauger, L. McAllister, E. Pajer, A. Westphal and G. Xu, JCAP **1006**, 009 (2010) [arXiv:0907.2916 [hep-th]]; M. Aich, D. K. Hazra, L. Sriramkumar and T. Souradeep, Phys. Rev. D **87**, 083526 (2013) [arXiv:1106.2798 [astro-ph.CO]]; D. K. Hazra, JCAP **1303**, 003 (2013) [arXiv:1210.7170 [astro-ph.CO]]; H. Peiris, R. Easther and R. Flauger, arXiv:1303.2616 [astro-ph.CO]; P. D. Meerburg and D. N. Spergel, Phys. Rev. D **89**, 063537 (2014) [arXiv:1308.3705 [astro-ph.CO]]; R. Easther and R. Flauger, arXiv:1308.3736 [astro-ph.CO].
- [51] J. Maldacena, JHEP **0305**, 013 (2003).
- [52] X. Chen, Adv. Astron. **2010**, 638979 (2010); X. Chen, R. Easther and E. A. Lim, JCAP **0706**, 023 (2007); JCAP **0804**, 010 (2008).
- [53] A. E. Romano and A. G. Cadavid, arXiv:1404.2985 [astro-ph.CO].
- [54] See <https://www.elisascience.org/>.

- [55] See <http://www.ligo.caltech.edu/>.
- [56] P. A. R. Ade *et al.* [The POLARBEAR Collaboration], arXiv:1403.2369 [astro-ph.CO].
- [57] D. Hanson *et al.* [SPTpol Collaboration], Phys. Rev. Lett. **111**, 141301 (2013) [arXiv:1307.5830 [astro-ph.CO]].
- [58] See http://lambda.gsfc.nasa.gov/product/map/dr3/m_products.cfm
- [59] See, <http://www.sciops.esa.int/index.php?project=planck&page=PlanckLegacyArchive>.
- [60] See http://bicepkeck.org/#data_products.